Using ^{210}Pb Simulations for model Comparison and analysing

Marco A Aquino-López[*†] Nicole K. Sanderson[‡] Maarten Blaauw[§]
J Andrés Christen[¶]

Abstract

Keywords: Plum, Age-depth models, Chronology, Constant Rate of Supply, Comparison.

[*]Centro de Investigación en Matemáticas (CIMAT), Jalisco s/n, Valenciana, 36023 Guanajuato, GT, Mexico. email: aquino@cimat.mx
[†]Corresponding author.
[‡]College of Life and Environmental Sciences, University of Exeter, Exeter, EX4-4QJ. email: N.K.Sanderson@exeter.ac.uk
[§]School of Natural and Built Environment, Queen's University Belfast, Belfast, BT7-1NN. email:maarten.blaauw@qub.ac.uk
[¶]Centro de Investigación en Matemáticas (CIMAT), Jalisco s/n, Valenciana, 36023 Guanajuato, GT, Mexico. email: jac@cimat.mx

1 Introduction

^{210}Pb is radioactive nuclide, which naturally forms in the atmosphere (as well as in the sediment) as result of the decay chain of ^{238}U. This isotope (with a half-life if 22.23 yr) is commonly used to date recent recent sediments (< 150 to 200 yr). Unlike other dating techniques such as ^{14}C, a single measurement of ^{210}Pb is useless for dating and it is only when a good portion of the decay curve is measured (together with certain assumptions about the sedimentation process) when a chronology can be established. In recent years palaeoecological and pollution studies have gain an increasing interest in the study of recent sediments in order to measure the human impact humans have in the environment. These studies strongly depend on the accuracy of the chronologies in order to correctly assign dates to chemical and biological changes.

The most commonly used model for dating recent sediment using ^{210}Pb is the Constant Rate of Supply (CRS) model (Appleby and Oldfield, 1978; Robbins, 1978; Sanchez-Cabeza and Ruiz-Fernández, 2012) also known as Constant Flux - CF model. This is not the only model but it is by far the most popular (see figure 1) and with most flexible assumptions. The CRS model assumes a constant supply of ^{210}Pb to the sediment from the atmosphere and allows for changes in the sedimentation rate. In order to estimate a chronology the CRS model uses a ratio between the complete inventory (the complete estimate of the radioactivity in the column of the sediment between the surface and a certain depth where ^{210}Pb from the atmosphere can no longer be found) and the remaining inventory from depth x ($t(x) = \frac{1}{\lambda}\log\left(\frac{A_0}{A_x}\right)$, where A_0 is the complete inventory, λ the decay constant of the $^{210}Pb \approx .03114$).

Other model requiere the assumption of constant supply of ^{210}Pb as well as other assumptions of the sedimentation process. The flexibility of the CRS, regarding its assumptions, comes at the cost of the need to measure a good portion of the inventory of the whole core or the use of interpolation in order to fairly estimate the complete inventory of ^{210}Pb in the sediment.

This model has received several revisions in order to improve its accuracy and applicability. There are two types of revisions to this model: revisions to its uncertainty (Binford, 1990; Sanchez-Cabeza et al., 2014) and to its applicability when extra information is available -extra dating sources e.g. ^{137}Cs or laminated sediments- (Appleby, 1998, 2001, 2008)

A recent study (Barsanti et al., 2020) an inter-laboratory presented a series of data to different laboratories around the world and each laboratory was ask to provide a chronology given the provided data. This experiment resulted in a whole range of different chronologies, given the same data. The different chronologies, not only because of the use of different models, but even when the same model was used different chronologies were obtained. The authors strongly advised to the use of independent time markers (extra dating sources) for the validation of the chronologies. This research clearly shows the effect that user decisions have on the resulting chronologies, which becomes extremely important when trying to replicate the resulting chronologies. User trying to replicate these chronologies will not only need access to the ordinal raw data but also to very user decision which lead to the resulting chronology, unfortunately these -raw data and decisions- are rarely reported.

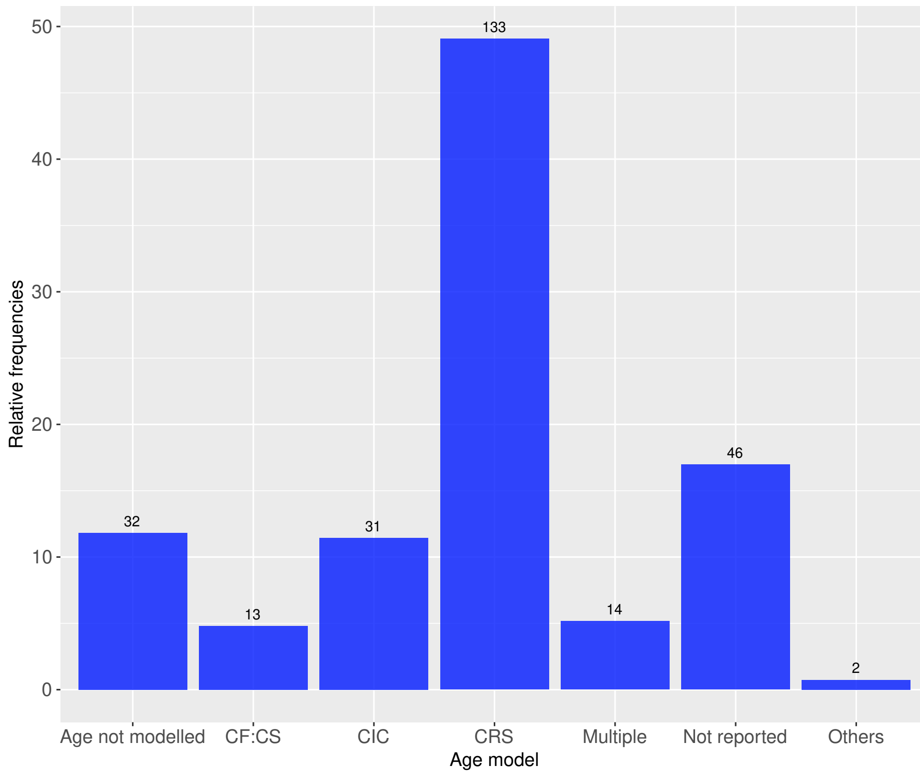

Figure 1: Models used in papers between 1964 and 2017. Data gather by Mustaphi et al. (2019) from literature review of 271 papers. CF:CS model also known as The Constant Flux - Constant Sedimentation (Robbins, 1978), CIC (Constant Initial Concentration) presented by Goldberg (1963); Crozaz et al. (1964); Robbins (1978), CRS - Constant Rate of Supply (Appleby and Oldfield, 1978; Robbins, 1978).

Recently Aquino-López et al. (2018) presented an alternative to these classical models, by introducing a Bayesian approach to the ^{210}Pb dating methodology, called *Plum*. This model treads every data point as originating from a system, which includes the sedimentation process as well as the decay process and it also incorporate an important variable to the infer process (the levels of supported ^{210}Pb - ^{210}Pb which naturally forms in the sediment and it normally threaded as a hindrance variable). Plum assumes that there exist a function $t(x)$ such that,

$$y_i \mid P_i^S, \Phi_i, \bar{t} \sim \mathcal{N}\left(A_i^S + \frac{\Phi_i}{\lambda}\left(e^{-\lambda t(x_i - \delta)} - e^{-\lambda t(x_i)} \right), (\sigma_i \rho_i)^2 \right). \tag{1}$$

where A_i^S is the supported ^{210}Pb in the sample, Φ_i the supply of ^{210}Pb to the sediment, δ the thickness of the sample and $t(x_i)$ the age of the sample at depth x_i. This treatment of the data allows for a formal statistical inference and by using a Bayesian approach all the parameters of the model can be infer. This differs from the CRS model because this last one uses the decay equation to obtained the age-depth function (which results in a more restrictive age-depth model) and does not provide a formal statistical inference. *Plum* has shown to provide accurate results with a realistic precision depending on the different case scenarios (Aquino-López et al., 2018, 2020) - both simulations and real cores. Under optimal conditions *Plum* and the CRS model have shown to provide similar results (Aquino-López et al., 2020) with *Plum* providing more realistic uncertainties, with minimal user interaction.

Blaauw et al. (2018) presented a comparison between classical and Bayesian age-depth models age-depth model construction. Blaauw concluded that Bayesian models provide a more accurate result and more realistic uncertainties under different scenarios - simulations and real core. In this study, we compre the CRS model (by far the most popular age-depth model for ^{210}Pb) against *Plum* under simulated cores. The objective of this analysis is to observe if the results that Blaauw et al. (2018) obtained are maintained on a more difficult situation as that of the construction of age-depth models using ^{210}Pb. We also want to observe the learning process of each of the models and how much information is needed to obtained a reasonable age-depth model given a particular model.

2 Simulations and Information Percentage

In order to observe the accuracy and precision of any model we need data to which the true age-depth function is known. Blaauw et al. (2018) presented a methodology for simulating radiocarbon dates and as their uncertainty, on the other hand Aquino-López et al. (2018) presented an approach for simulating ^{210}Pb data given a age-depth function $f(t)$. it is important to note that these simulations follow the equations presented by Appleby and Oldfield (1978); Robbins (1978) guaranteeing that the CRS assumptions are meet. By using the approach presented by Aquino-López et al. (2018) for simulating ^{210}Pb data and the structure of uncertainty estimation presented by Blaauw et al. (2018), resalable ^{210}Pb simulated data can be obtained.

2.1 Simulation Construction

Three different proposals (see table 2.1) were chosen for our simulations, each with their own age-depth functions. This scenarios were selected as they provide three challenges for the models: the first proposal presents a age-depth function which is quite common for recent sediments, the second proposal presents challenging core as the function replicates a drastic and quick change in sediment behaviour around depth 15 cm, lastly proposal three presents a cyclic and periodic change in accumulation. Using the age-depth functions and defined parameters in table 2.1, we can obtained simulate the activity at any depth or interval (by integrating the curve in such interval).

These concentrations (see Figure 2) can be interpreted as error-free measurements. Because every equipment is subject to error, we need to replicate this measurement errors. Blaauw et al. (2018) presents error structure for radiocarbon dates. We can use this structure to our ^{210}Pb measurements as both measurements

Label	Age-depth function	Φ $(\frac{Bq}{m^2 yr})$	Supported ^{210}Pb $(\frac{Bq}{kg})$
Proposal 1	$\frac{x^2}{4}+\frac{x}{2}$	100	10
Proposal 2	$12x - .2x^2$	50	25
Proposal 3	$8x + 25\sin(\frac{x}{\pi})$	500	15

Table 1: Simulated age-depth function and parameters used in each simulation

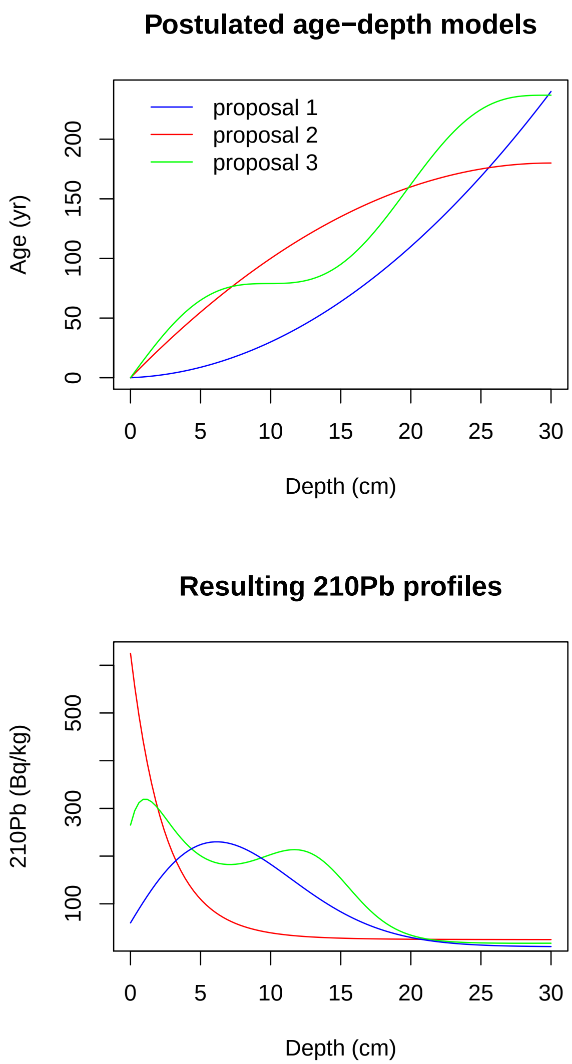

Figure 2: Proposed age-depth functions with their corresponding ^{210}Pb profiles. Upper panel: Age-depth function for the three different proposals. Lower panel: Corresponding ^{210}Pb profiles in relation to depth.

are subject to similar measurement problems.

Let $C_{\hat{x}}$ be the true ^{210}Pb concentration in the interval $\hat{x} = [a, b)$, given the age-depth function $t(x)$ and parameters Φ and A^S. To simulate disturbances in the material, we can introduce scatter centred around the true value, $\theta \sim \mathcal{N}\left(C_{\hat{x}}, y^2_{scat}\right)$, where x^2_{scat} is the amount of scatter for this variable (in this case $y^2_{scat} = 10$). Now, to replicate outliers, a shift from the true value (x_{shift}) is defined, which occurs with a probability p_{out}. This results in a new variable θ' which is defined as

$$\theta' = \begin{cases} \mathcal{U}(\theta - x_{shift}, \theta + x_{shift}), & p_{out} \\ \theta, & 1 - p_{out} \end{cases}. \tag{2}$$

To simulate the uncertainty provided by the laboratory, we can define the simulated measurements as $y(\theta') \sim \mathcal{N}\left(\mu(\theta'), \sigma^2_R\right)$, where σ_R is the standard deviation reported by the laboratory. σ_R is defined as $\sigma_R = \max\left(\sigma_{min}, \mu(\theta')\ \varepsilon\ y_{scat}\ \right)$, where σ_{min} is the minimum standard deviation assigned to a measurement. This variable differs between laboratories (we will be using a default value of 1 Bq/kg). Finally, ε is the analytical uncertainty (default .01) and y_{scat} an error multiplier (default 1.5).

For this this study we created a data set for each simulation by integrating in intervals of 1 cm from depth 0 to 30 (where equilibrium was guaranteed). The complete data sets can be found in the Supplementary Material 5 and Figure 2 shows the ^{210}Pb concentrations curves with their corresponding age-depth functions.

2.2 Percentage of information

With these base data sets, we then define a new variable call percentage of information. This variable relates to how many much of the available information was measured. We assumed that background was reached at depth m, information percentage is define as how much area of the core was measured, e.g. if background was reached at depth 100 cm and the core was sampled very 1 cm if 20 samples are measured, the percentage of information would be 20 %. This variable will help us to have a measuring tool for how many samples are needed for a good chronology without depending on the size of the samples.

In order to compare both the CRS and *Plum* under simular circumstances, the previously described data sets will be randomly selected for samples given a information percentage. In the case of cores which have not reach background, *Plum* (Aquino-López et al., 2018) has shown to provide accurate results without the need of user interference, on the other hand, the CRS can provide a chronology if inventory is estimating using extrapolation and forcing the model to pass by a known date. This means user innervation and to avoid this problem and to provide a more objective comparison, every sampling set will reach background, which guaranties the proper use of the CRS model.

3 Model Comparison

To allow for a reasonable comparison between model and to observe the effect that different percentage of information have on the accuracy and precision of ^{210}Pb models, we used the three simulated data sets created for the previous section. This simulated cores were randomly selected given a percentage of information (e.g. for a 20% information sample, in the 30 cm cores, 6 random samples were selected). Becase the CRS model assumes that background has being reached (In order to reduce user manipulation), we decided to fix the last sample (30 cm depth) for every case. This guaranties the proper use of the CRS model and also gives the model a single last depth to be removed as it is common practice when using this model. 100 different samples were randomly selected for information percentages from 10% to 95% in a 5% intervals (e.i 10%, 15%, 20%,...,95%) and the complete sample was also used i.e 100% percentage of information. After a random sample was selected, both the CRS model and *Plum* were performed and compared to the true age value to calculate its accuracy. *Plum* was run using the default settings.

In order to observe the precision and accuracy, we decided to calculate the offset (in yr), the mean of length of the 95% intervals (in yr), as well as the normalized accuracy (this variable will show us how far the model is from the true value given its own uncertainty).

Figure 3 show similar results those presented by Blaauw et al. (2018). The classical model (CRS) at first appears to provide a similar result (similar offset) to the Bayesian alternative (*Plum*) with a more precise results (if we only look at the length of the 95% interval). These results can be misleading if we don't analysed the effects of these two parameters in together (offset and length of interval). To have a more realistic representation of how the models capture the true values age-depth models we can observe the normalized offset. This variable (normalized offset) shows how on average the models contain the true within their uncertainty intervals (normalized to one standard deviation). Any model which normalized offset is bigger than two (two standard deviations) is incapable of capturing the true ages within their uncertainty intervals. This means that the CRS provides smaller uncertainties at the cost of its accuracy. It also appears that the length of the 95% interval and offset is not affected by how much information is provided to the model.

On the other hand, *Plum*, which is a Bayesian method, shows more accurate results as more information is given to the model, this again coincides with the results found in Blaauw et al. (2018). When we observe the regular offset (not normalized), we observed that Plum provides a smaller offset in comparison to the CRS model, this in combination with slightly bigger uncertainties results on a consistently accurate model which is capable of capturing the true values within its uncertainty intervals. This result supports the clame that *Plum* provides more realistic uncertainties when compared to the CRS.

Another important statistic to take into account is that, *Plum* has 87.86% (4686/5333) of its runs under the 2 standard deviations, on the other hand the CRS model only has 7.48% (399/5333) and only .54% (29/5333) lies under the 1 standard deviation, which is the most commonly reported interval when reporting

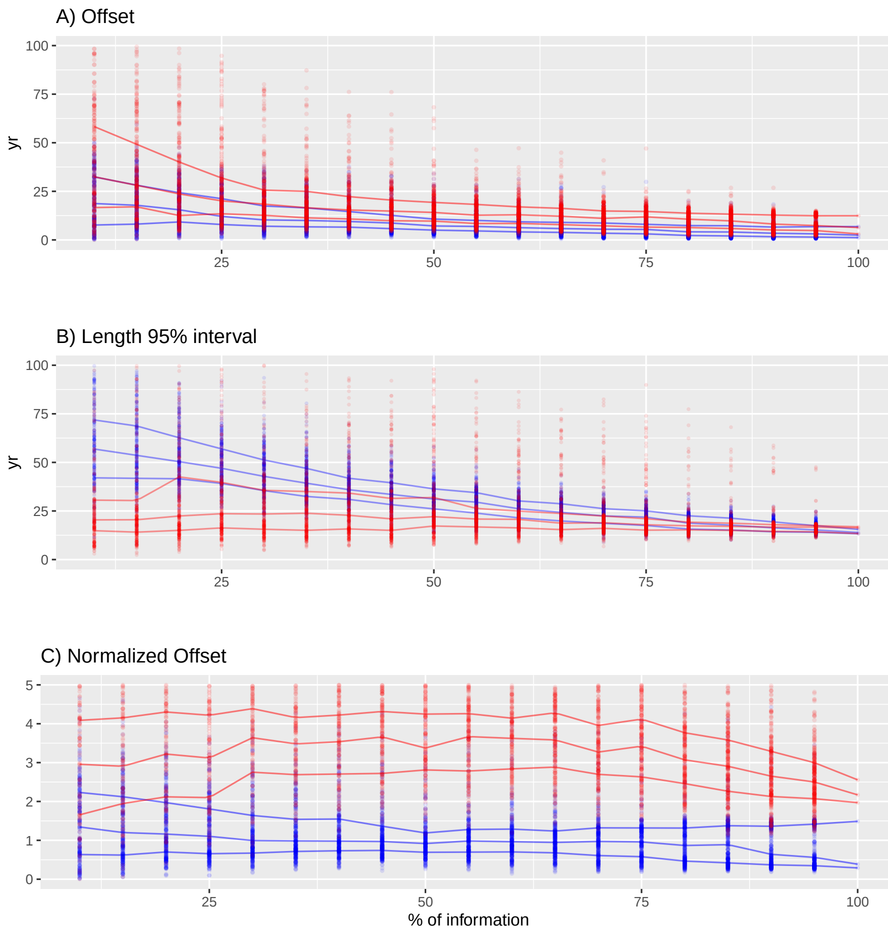

Figure 3: Comparison of the offset (distance between the true age and model), the lenght of the 95% confidence interval (classical) and credible interval (Bayesian) and the Normalized offset between the classical CRS model vs the Bayesian approach *Plum*. Top panel A) shows the offset between the true age and modelled age of the CRS (red) and *Plum* (blue). Middle panel B) length of the 95% confidence interval for the CRS model (in red) and the 95% credible interval of *Plum* (in blue). Bottom panel C) Normalized offset presenting the distance between the modelled age and the true age normalized divided by the standard deviation (in the case of *Plum*, the length of the interval divided by 4), CRS in red and *Plum* in blue.

CRS results. We can also observe a clear structure on the way Plum increases its accuracy and precision to obtained a better chronology as more information is available, on the side the CRS model appears to not have this structure. This results are presented for the overall chronology (the mean offset, interval and normalized offset of the overall chronology). In order to observe if certain model is better predicting a certain section of the sediment we have to look at the normalized offset of every depth.

Figure 4 shows the normalized accuracy of every simulation by depth for both models. It is clear than *Plum* shows a clear depending which depends on the information available to the model. The information percentage appears to be irrelevant to the accuracy of the CRS model, contrary to the results obtained by *Plum*. It is important to note that the inaccuracies of the CRS model are not exclusive to any particular sections of the chronology, this is most likely cause by the small uncertainties provided by the model.

4 Conclusions and Discussion

These results show a clear bias provided by the CRS model. Aquino-López et al. (2018) discussed this point and states that the bias is the product of the use of a logarithmic function for the age-depth function. It is also evident from these results that the CRS model's uncertainties are not sufficient to capture the true age-depth function. This is an important point given the fact that is common practice amount the ^{210}Pb dating community to report credible intervals to one single deviation (instad of the 95% confidence intervals, which are common practice in most other fields). Other confidence intervals can be calculated for this model (Sanchez-Cabeza et al., 2014) but the fact that this intervals are even smaller than the ones obtained by error propagation (Appleby, 2001) is of consent.

Previous work on model comparison (Barsanti et al., 2020) have shown the problems with the variability of ^{210}Pb results even when different users apply the same or similar models to a single set of data. In this work, user input was reduced to the minimal as an effort to show the effects of different information percentages have in the resulting chronology. The results of this experiment showed that the CRS model can provide extremely different results even when the data originates from the same data set. Figure 3 showed that the CRS model appears to dont learn from using more data. This is explains why over the years, many authors have insisted in the use of other dating techniques to validate the chronology provided by the CRS (Sanchez-Cabeza and Ruiz-Fernández, 2012; Barsanti et al., 2020; Aquino-López et al., 2020). These results highly encourage the need of validating the CRS chronology before it is use.

On the other hand, *Plum* shows a consistent accurate result by capturing the true values within the 95% credible intervals on a more constant matter. It is important to note that one of the big advantages of *Plum* is its increasing accuracy and precision reduction as more data becomes available. In the case of proposal 2, we observe that *Plum* appears to behaves worse as more data is available, this would be of concern if we do not take into consideration that this proposal was extremely inusual on the real world and also if user would not double check the resulting chronologies. If more information is available about the core or the

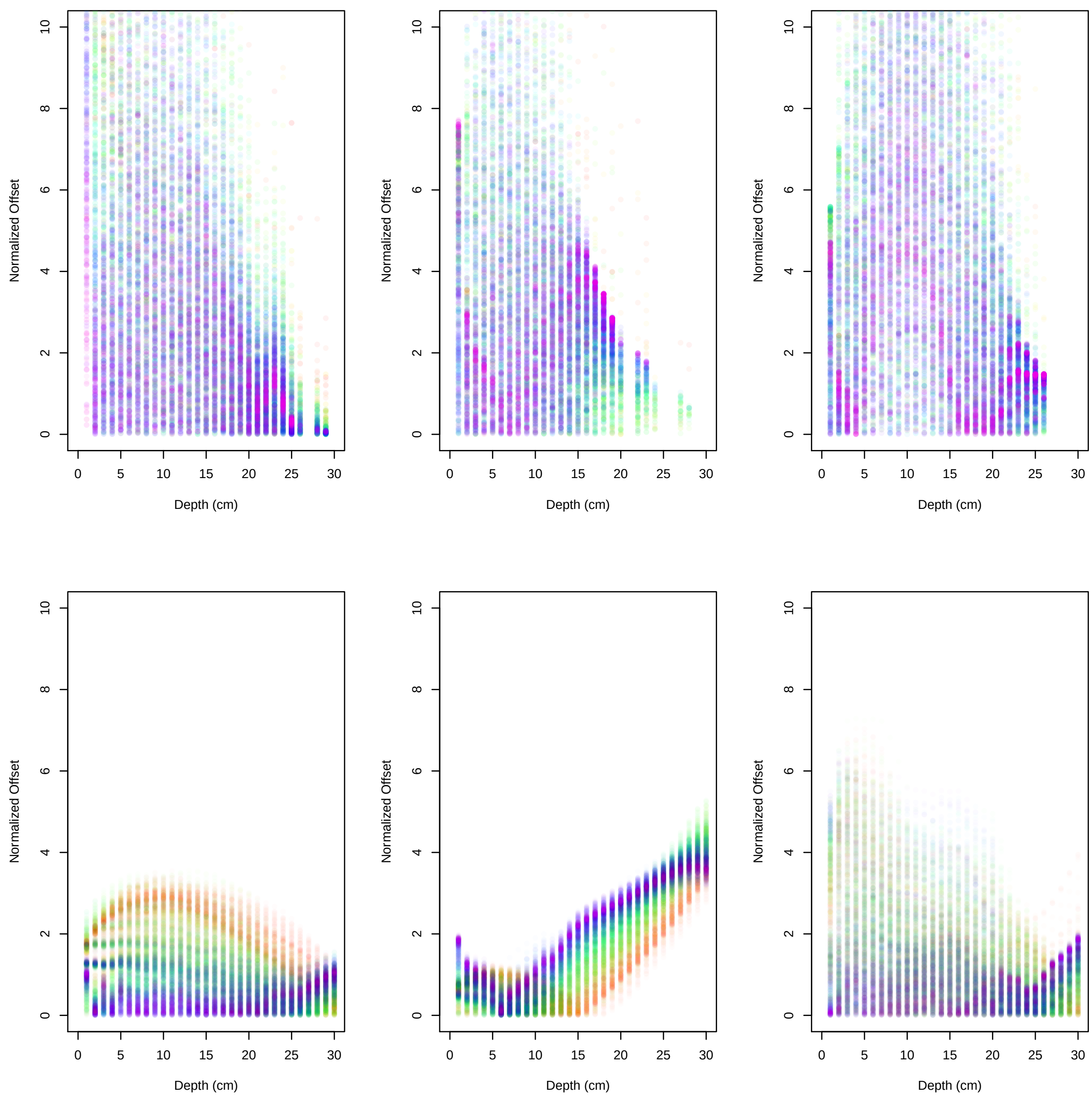

Figure 4: Normalized accuracy of every simulation at very depth. Red dots represent the low information percentage samples and purple dots represent high percetange samples. Top figures are the normalized offset of the CRS model as the bottom ones are the results for *Plum*. Columns from left to right show the results for proposal 1, 2 and 3.

sediment, this information can easily be implemente as prior information in *Plum*, this will result in a much better chronology. It is also important to note that even when *Plum* performs badly on this specific case it is providing a much better chronology to the first 10-15 cm of the core compared to the CRS model which dating is chaotic.

In conclusion, we recommend that users validate their chronology when possible, and it not extra information is available for this validation, we recommend them to use the Bayesian approach and provide it with as much information as it would be possible. This will guaranties that they they get the best possible chronology

References

Appleby, P. (2008). Three decades of dating recent sediments by fallout radionuclides: a review. *The Holocene*, 18(1):83–93.

Appleby, P. and Oldfield, F. (1978). The calculation of lead-210 dates assuming a constant rate of supply of unsupported 210pb to the sediment. *Catena*, 5(1):1–8.

Appleby, P. G. (1998). Dating recent sediments by Pb-210: Problems and solutions. *Proc. 2nd NKS/EKO-1 Seminar, Helsinki, 2-4 April 1997, STUK, Helsinki*, pages 7–24.

Appleby, P. G. (2001). Chronostratigraphic techniques in recent sediments. *Tracking Environmental Change Using Lake Sediments: Basin Analysis, Coring, and Chronological Techniques*, pages "171–203".

Aquino-López, M. A., Blaauw, M., Christen, J. A., and Sanderson, N. K. (2018). Bayesian analysis of 210pb dating. *Journal of Agricultural, Biological and Environmental Statistics*, 23(3):317–333.

Aquino-López, M. A., Ruiz-Fernández, A. C., Blaauw, M., and Sanchez-Cabeza, J.-A. (2020). Comparing classical and bayesian 210pb dating models in human-impacted aquatic environments. *Quaternary Geochronology*, 60:101106.

Barsanti, M., Garcia-Tenorio, R., Schirone, A., Rozmaric, M., Ruiz-Fernández, A., Sanchez-Cabeza, J., Delbono, I., Conte, F., Godoy, J. D. O., Heijnis, H., Eriksson, M., Hatje, V., Laissaoui, A., Nguyen, H., Okuku, E., Al-Rousan, S. A., Uddin, S., Yii, M., and Osvath, I. (2020). Challenges and limitations of the 210pb sediment dating method: Results from an IAEA modelling interlaboratory comparison exercise. *Quaternary Geochronology*, 59:101093.

Binford, M. W. (1990). Calculation and uncertainty analysis of ^{210}Pb dates for PIRLA project lake sediment cores. *Journal of Paleolimnology*, 3:253–267.

Blaauw, M., Christen, J. A., Bennett, K., and Reimer, P. J. (2018). Double the dates and go for Bayes — impacts of model choice, dating density and quality on chronologies. *Quaternary Science Reviews*, 188:58–66.

Crozaz, G., Picciotto, E., and de Breuck, W. (1964). Antarctic snow chronology with pb210. *Journal of Geophysical Research*, 69(12):2597–2604.

Goldberg, E. D. (1963). Geochronology with pb-210. *Radioactive Dating*, pages 121–131.

Mustaphi, C. J. C., Brahney, J., Aquino-López, M. A., Goring, S., Orton, K., Noronha, A., Czaplewski, J., Asena, Q., Paton, S., and Brushworth, J. P. (2019). Guidelines for reporting and archiving 210pb sediment chronologies to improve fidelity and extend data lifecycle. *Quaternary Geochronology*, 52:77–87.

Robbins, J. (1978). Geochemical and geophysical applications of radioactive lead. *The biogeochemistry of lead in the environment*, pages 285–393.

Sanchez-Cabeza, J. A. and Ruiz-Fernández, A. C. (2012). 210Pb sediment radiochronology: An integrated formulation and classification of dating models. *Geochimica et Cosmochimica Acta*, 82:183–200.

Sanchez-Cabeza, J. A., Ruiz-Fernández, A. C., Ontiveros-Cuadras, J. F., Pérez Bernal, L. H., and Olid, C. (2014). Monte Carlo uncertainty calculation of 210Pb chronologies and accumulation rates of sediments and peat bogs. *Quaternary Geochronology*, 23:80–93.

5 Supplementary Material

Data for each simulation is hosted at (add github here)

Label	Depth (cm)	Density (g/cm^3)	210Pb (Bq/kg)	sd(210Pb)	Thickness (cm)	226Ra (Bq/kg)	sd(226Ra)
Sim01-01	1	0.10009	63.50103	2.85755	1	23.8045	1.125
Sim01-02	2	0.10064	80.08738	3.60393	1	23.2924	1.125
Sim01-03	3	0.10173	98.32806	4.42476	1	23.434	1.125
Sim01-04	4	0.10334	125.45705	5.64557	1	26.0873	1.125
Sim01-05	5	0.10547	141.27971	6.35759	1	22.8041	1.125
Sim01-06	6	0.10809	130.27571	5.86241	1	23.4333	1.125
Sim01-07	7	0.11116	134.04051	6.03182	1	25.6156	1.125
Sim01-08	8	0.11466	129.69245	5.83616	1	26.1371	1.125
Sim01-09	9	0.11855	134.93655	6.07214	1	25.4813	1.125
Sim01-10	10	0.12278	109.39886	4.92295	1	25.8877	1.125
Sim01-11	11	0.12731	110.68133	4.98066	1	24.4414	1.125
Sim01-12	12	0.13209	102.38094	4.60714	1	24.9053	1.125
Sim01-13	13	0.13706	75.80895	3.4114	1	22.9151	1.125
Sim01-14	14	0.14218	77.60406	3.49218	1	24.4808	1.125
Sim01-15	15	0.14738	68.4401	3.0798	1	24.9343	1.125
Sim01-16	16	0.15262	60.72037	2.73242	1	25.2659	1.125
Sim01-17	17	0.15782	50.28147	2.26267	1	22.961	1.125
Sim01-18	18	0.16294	44.24641	1.99109	1	22.9139	1.125
Sim01-19	19	0.16791	39.85997	1.7937	1	28.3774	1.125
Sim01-20	20	0.17269	38.40823	1.72837	1	23.5379	1.125
Sim01-21	21	0.17722	32.75922	1.47416	1	25.4363	1.125
Sim01-22	22	0.18145	28.02545	1.26115	1	24.8995	1.125
Sim01-23	23	0.18534	27.8749	1.25437	1	22.6783	1.125
Sim01-24	24	0.18884	30.74797	1.38366	1	24.8575	1.125
Sim01-25	25	0.19191	28.36187	1.27628	1	24.8724	1.125
Sim01-26	26	0.19453	27.24535	1.22604	1	24.3778	1.125
Sim01-27	27	0.19666	23.59236	1.06166	1	24.7209	1.125
Sim01-28	28	0.19827	25.74855	1.15868	1	24.6615	1.125
Sim01-29	29	0.19936	25.05368	1.12742	1	24.7199	1.125
Sim01-30	30	0.19991	25.0065	1.12529	1	24.4937	1.125

Label	Depth (cm)	Density (g/cm^3)	210Pb (Bq/kg)	sd(210Pb)	Thickness (cm)	226Ra (Bq/kg)	sd(226Ra)
Sim02-01	1	0.1001	909.3928	40.9227	1	8.9761	0.45
Sim02-02	2	0.1006	683.9989	30.7799	1	10.0607	0.45
Sim02-03	3	0.1017	453.0503	20.3873	1	9.8701	0.45
Sim02-04	4	0.1033	310.7897	13.9855	1	10.37	0.45
Sim02-05	5	0.1055	218.0058	9.8103	1	10.0418	0.45
Sim02-06	6	0.1081	158.6974	7.1414	1	10.104	0.45
Sim02-07	7	0.1112	113.9062	5.1258	1	10.2049	0.45
Sim02-08	8	0.1147	75.5493	3.3997	1	9.334	0.45
Sim02-09	9	0.1185	56.6252	2.5481	1	10.5145	0.45
Sim02-10	10	0.1228	44.1595	1.9872	1	9.8677	0.45
Sim02-11	11	0.1273	34.7448	1.5635	1	9.7694	0.45
Sim02-12	12	0.1321	25.384	1.1423	1	10.5134	0.45
Sim02-13	13	0.1371	24.0007	1.08	1	10.4589	0.45
Sim02-14	14	0.1422	21.3643	1	1	9.9504	0.45
Sim02-15	15	0.1474	17.7932	1	1	10.5135	0.45
Sim02-16	16	0.1526	15.0416	1	1	10.3362	0.45
Sim02-17	17	0.1578	14.2937	1	1	10.5131	0.45
Sim02-18	18	0.1629	12.3844	1	1	10.368	0.45
Sim02-19	19	0.1679	12.6023	1	1	10.5297	0.45
Sim02-20	20	0.1727	11.9329	1	1	10.0924	0.45
Sim02-21	21	0.1772	9.301	1	1	10.118	0.45
Sim02-22	22	0.1815	10.7777	1	1	10.249	0.45
Sim02-23	23	0.1853	12.9491	1	1	10.134	0.45
Sim02-24	24	0.1888	10.6571	1	1	10.1151	0.45
Sim02-25	25	0.1919	9.6297	1	1	9.6608	0.45
Sim02-26	26	0.1945	8.4331	1	1	8.7821	0.45
Sim02-27	27	0.1967	10.4921	1	1	9.8995	0.45
Sim02-28	28	0.1983	11.135	1	1	9.2481	0.45
Sim02-29	29	0.1994	10.109	1	1	10.4398	0.45
Sim02-30	30	0.1999	9.5404	1	1	10.1114	0.45

Label	Depth (cm)	Density (g/cm^3)	210Pb (Bq/kg)	sd(210Pb)	Thickness (cm)	226Ra (Bq/kg)	sd(226Ra)
Sim03-01	1	0.1001	6384.1354	287.2861	1	15.8007	0.675
Sim03-02	2	0.1006	3550.0809	159.7536	1	14.5245	0.675
Sim03-03	3	0.1017	1954.5702	87.9557	1	15.6527	0.675
Sim03-04	4	0.1033	1183.8917	53.2751	1	14.5175	0.675
Sim03-05	5	0.1055	760.2132	34.2096	1	14.9242	0.675
Sim03-06	6	0.1081	360.2553	16.2115	1	14.801	0.675
Sim03-07	7	0.1112	212.9402	9.5823	1	14.8738	0.675
Sim03-08	8	0.1147	104.2684	4.6921	1	14.9028	0.675
Sim03-09	9	0.1185	44.3849	1.9973	1	15.0768	0.675
Sim03-10	10	0.1228	18.6447	1	1	15.3764	0.675
Sim03-11	11	0.1273	23.2778	1.0475	1	14.6231	0.675
Sim03-12	12	0.1321	53.1587	2.3921	1	15.1629	0.675
Sim03-13	13	0.1371	97.363	4.3813	1	14.3047	0.675
Sim03-14	14	0.1422	116.9788	5.264	1	14.0261	0.675
Sim03-15	15	0.1474	153.2901	6.8981	1	15.9723	0.675
Sim03-16	16	0.1526	151.8496	6.8332	1	14.7579	0.675
Sim03-17	17	0.1578	136.3609	6.1362	1	16.114	0.675
Sim03-18	18	0.1629	107.2736	4.8273	1	15.4595	0.675
Sim03-19	19	0.1679	76.8966	3.4603	1	15.9439	0.675
Sim03-20	20	0.1727	48.9213	2.2015	1	14.6235	0.675
Sim03-21	21	0.1772	40.4439	1.82	1	14.6716	0.675
Sim03-22	22	0.1815	26.5638	1.1954	1	16.2541	0.675
Sim03-23	23	0.1853	21.714	1	1	14.4826	0.675
Sim03-24	24	0.1888	17.6428	1	1	15.5109	0.675
Sim03-25	25	0.1919	17.3533	1	1	13.6898	0.675
Sim03-26	26	0.1945	17.4211	1	1	14.4684	0.675
Sim03-27	27	0.1967	16.4246	1	1	15.3889	0.675
Sim03-28	28	0.1983	12.4828	1	1	15.0698	0.675
Sim03-29	29	0.1994	13.5514	1	1	15.2346	0.675
Sim03-30	30	0.1999	14.3145	1	1	14.7846	0.675